EGU2020-10128

Wind estimates in the mesosphere - lower thermosphere retrieved from infrasound data

Ekaterina Vorobeva[1] (ekaterina.vorobeva@ntnu.no), Sven Peter Näsholm[2], Patrick Espy[1], Yvan Orsolini[3], Robert Hibbins[1]

[1] Norwegian University of Science and Technology, Trondheim, Norway

[2] NORSAR, Kjeller, Norway

[3] Norwegian Institute for Air Research, Kjeller, Norway

Abstract

We analyze dataset of infrasound observations from surface military explosions in Hukkakero, northern Finland which occur yearly in August and September since 1988. The transient nature of these events allows for identification of returns reflected (or scattered) both from stratospheric and from mesospheric - lower thermospheric (MLT) altitudes. The infrasound data were recorded at Norwegian infrasound-array station around 200 km north of the explosion site. In this study, we use the measured travel-time and backazimuth deviation of the arriving infrasound wavefronts to estimate the MLT cross-wind averaged along the propagation path. The spatial extent of that averaging process is explored, and the MLT wind estimates retrieved from infrasound data are presented and compared against high-top atmospheric model winds.

Infrasound array

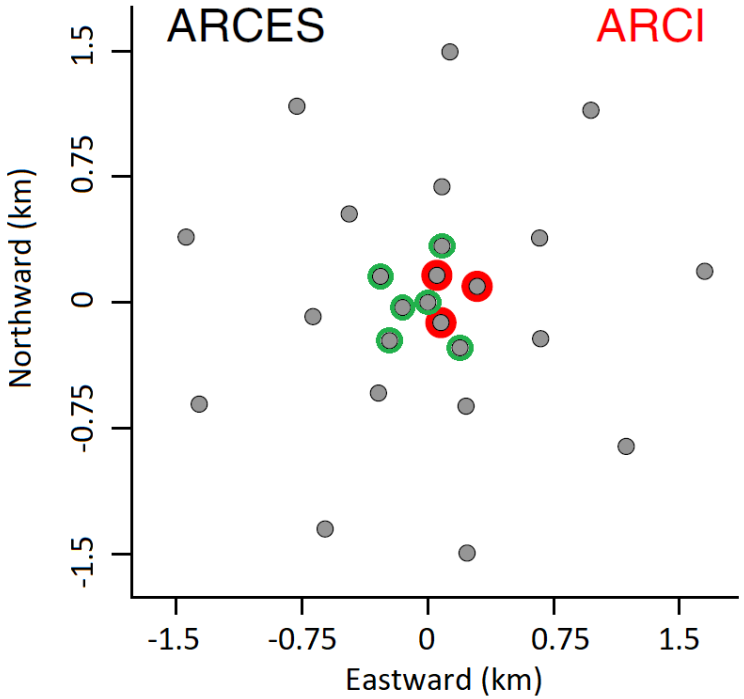

Figure 1. The geometry of the ARCES (69.5 N, 25.5 E) seismic array (grey) and ARCI infrasound array (red - 2008-2010; green and red - present). Adapted from [Evers and Schweitzer, 2011].

The co-located ARCES/ARCI arrays (69.53 N, 25.51 E) are located in northern Norway (Figure 1). ARCES is the ground-based seismic array operating since 1987 which has 25 elements and aperture of 3 km. **ARCI** is the experimental infrasound array operating since 2008 and initially containing three-elements with 150 m aperture (Figure 1). The ARCI has been gradually expanded and now has 9 elements.

The infrasound array is located 178 km to the North from the site where surface military explosions take place. Explosions occur yearly in August and September since 1988. In this study, analysis for 3 years of data 2008-2010 is performed.

For further analysis data are filtered using band-pass filter to **0.4 – 1 Hz** in order to remove microbarom signal but be able to look at low-frequency arrivals from the MLT region [Hedlin et al., 2012].

Parameters used in this study are measured travel-time and backazimuth deviation (uncertainty of 5° [Evers and Schweitzer, 2011]) of the arriving infrasound wavefronts.

Methodology of cross-wind estimation

1. Cross-wind estimation in a layer

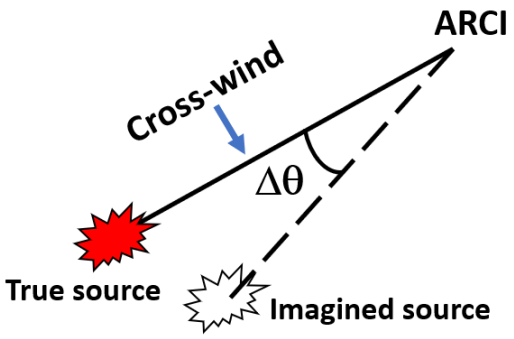

Figure 2. To the explanation of cross-wind estimation.

Further consideration is held in right-handed coordinate system where y axis is positive in the direction of wave front propagation and z axis is positive upward. Propagating upward from the source, a wave front is affected by atmospheric wind. The result of such influence is deviation of the observed direction of arrival (backazimuth) from the true one $\Delta\theta = \theta_{true} - \theta_{obs}$ (Figure 2). In this study, the source location is known as well as explosion onsets, and this allows to estimate the cross-wind effect along the propagation path (Diamond, 1984; Blixt et al., 2019):

$$w_{c,T} = \frac{D}{T}\tan(\Delta\theta) \quad (1)$$

where D is the great-circle distance between the source and the receiver, T is measured total travel time.

Based on time delay between arrivals from altitude *i* and altitude *j*, it is possible to use the following analog of Eq (1) to estimate **the average cross-wind effect in a layer**:

$$w_{c,Tij} = \frac{D}{T_j - T_i}\left[\tan(\Delta\theta_j) - \tan(\Delta\theta_i)\right]. \quad (2)$$

Surface military explosions in northern Finland occur yearly in August and September since 1988. The transient nature of these events allows for identification of returns reflected (or scattered) both from stratospheric (typically 10 – 13 min after

onset for Hukkakero-ARCI geometry) and from MLT (13 – 17 min after onset) altitudes. Thus, Eq (2) can be applied to estimate the average cross-wind in the troposphere-stratosphere if $T_i = 0$, $\Delta\theta_i = 0$ (Blixt et al., 2019) as well as the the average cross-wind in the MLT region if T_i is travel time of detected arrival from stratospheric region, and $\Delta\theta_i$ is the corresponded backazimuth deviation.

Eq. (1) lets to retrieve information about atmospheric winds based on ground-based observations and is currently used [Diamond, 1964; Blixt et al., 2019; Amenzua et al., 2020].

2. Uncertainty

Cross-wind can be considered as a function of two variables T and θ_{obs}, since the distance between the source and the receiver as well as true backazimuth are constant and are not affected by atmospheric wind. Thus, it is possible to estimate the relative uncertainty of cross-wind based on variables' uncertainties. Since cross-wind is a function of two variables and we want to look at max possible range of cross-wind uncertainty, the sensitivity analysis (error propagation) is used in this study. The expression for the relative uncertainty of cross-wind is

$$\frac{\partial w_{cross}}{w_{cross}} = \sqrt{\left(\frac{\partial T}{T}\right)^2 + \left(\frac{\partial \theta_{obs}}{\Delta\theta}\right)^2}. \qquad (3)$$

Following [Blixt et al., 2019], assume travel-time uncertainty $\partial T = 10$ s. Note that this study is focused on wind in the middle atmosphere which implies that the wave front takes minutes to reach 30 – 100 km altitude and return back to the ground. Hence the contribution of the travel-time uncertainty to the uncertainty of cross-wind is negligible, and contribution from uncertainties of observed backazimuth (measurement uncertainty) and backazimuth deviation (wind power) dominate.

Comparison with the atmospheric model

The comparison of main model parameters for two global scale atmospheric models, CMAM [Fomichev et al., 2002] and WACCM-X [Liu et al., 2018], is shown in Table 1. Both models are nudged by reanalysis data below 50 km: ERA-Interim (CMAM) and MERRA (WACCM-X). In this study, the **WACCM-X is used** for comparison with infrasound observations since it has better spatial and temporal resolution. Figure 3 presents the source-receiver location on the model grid.

Table 1.Model parameters.

	Ext-CMAM	WACCM-X
$\Delta x \times \Delta y$	6°× 6°	2.5° × 1.9°
Δt	6h	1h
p levels	87	145
z_{top}	~210km	~500km

We extract zonal wind, meridional wind and temperature from the grid node closest to **a)** the midpoint between the source and the receiver and **b)** the explosion onset + 10 min.

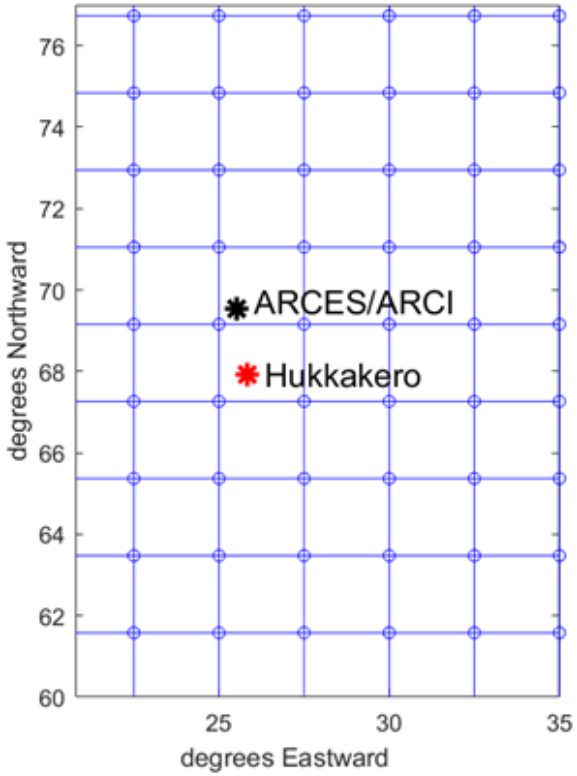

Figure 3. The source-receiver location on the WACCM-X grid.

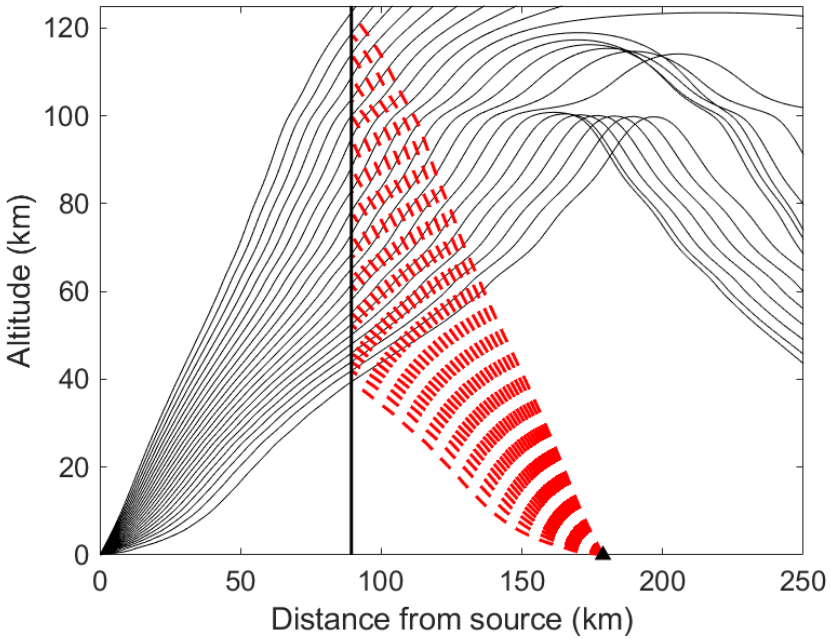

Figure 4. An example of ray propagation modelling. Ray tracing results (black) and assumed propagation path after scattering (red).

To compare model wind with infrasound observations, we need to know in what layer to average model wind. In other words, it is necessary to estimate altitude at which scattering occurs. For this, a ray propagation through the atmosphere is simulated using GeoAc ray tracing model and u, v, T profiles extracted from the WACCM-X model.

The infrasound array is located in the shadow zone, so ray tracing does not predict arrivals at ACRI. Despite this, 99% of the explosions might be observed in the data [Blixt et al., 2019]. It lets us assume scattering or partial reflection at the midpoint between the source and the receiver (Figure 4).

Comparing the measured travel time with time predicted by the ray tracing model, it is possible to estimate altitude at which scattering occurs. Next, for a given ray path, average over propagation path cross-wind can be extracted from the model data as travel-time weighted sum of cross-winds.

Results

The analysis has been performed based on detections at ARCI array in August-September 2008 – 2010. Total number of explosions is 81. Only well-detected wave front arrivals (with averaged correlation between traces > 0.5) are considered.

Obtained results are shown in Figure 5 and Table 2 and will be discussed in the next section.

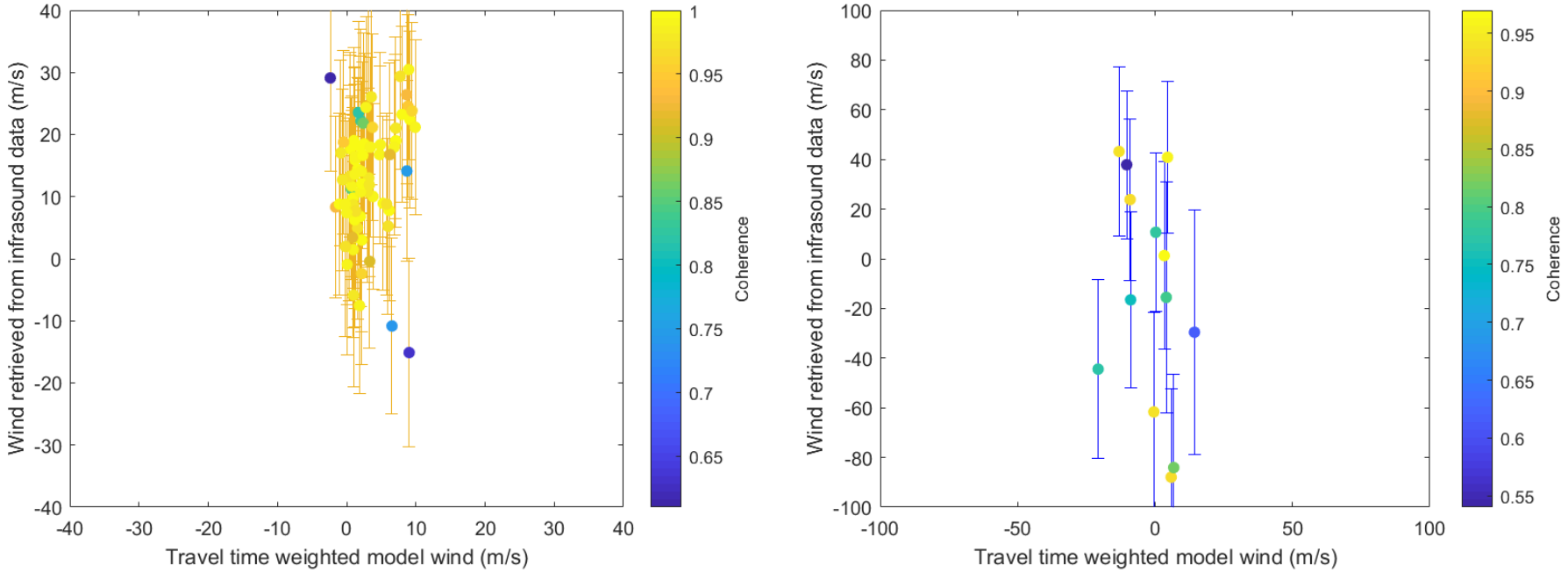

Figure 5. The average cross-wind estimated from WACCM-X data (horizontal axis) against average cross-wind from infrasound observations at ARCI array calculated using Eq. 2 (vertical axis) for 81 explosions in 2008 – 2010. Left - wind estimates for stratospheric arrivals. Right – wind estimates for MLT arrivals.

Discussion

- Returns reflected (or scattered) back from the altitude of about 40 km are observed more often in contrast with returns from higher altitudes (Table 2).
- Average cross-wind retrieved from infrasound observations is much stronger in the MLT region than in the troposphere-stratosphere. That agrees with our understanding of the atmospheric dynamics (Figure 6).
- As a rule, backazimuth deviation for stratospheric arrivals is positive and small. That means that average effect of cross-wind over first 40 km is eastward and weak (0 – 20 m/s). This result is in agreement with the behavior of zonal wind field at mid latitudes in transition period between summer and winter when seasonal reversal from easterlies to westerlies occurs (Figure 6).
- In the same time, backazimuth deviation for MLT arrivals change sign and vary in wider limits. That agrees with behavior of the wave driven MLT region during the transition period when the semidiurnal tide is strong and a mix of modes (migrating + non-migrating).

Table 2. Analysis results.

Arrival	Stratospheric	MLT
Number of detections at pressure sensors (ARCI)	77	13
Number of detections with $\Delta\theta > 0$	70	6
Number of detections with $\Delta\theta < 0$	7	7
Typical altitude of reflection	44 km	100 km

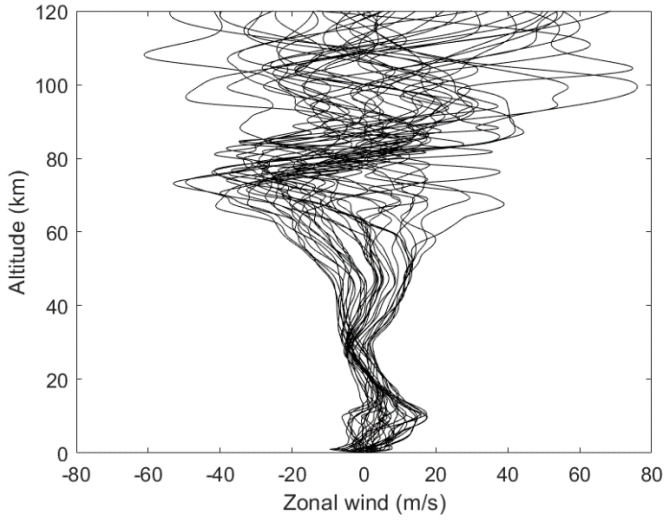

Figure 6. zonal wind profiles extracted from the WACCM-X for time node closest to the explosion onset are shown for 36 incidents in 2008 during August-September.

Acknowledgments

The research is supported by the Research Council of Norway FRIPRO/FRINATEK basic research programme, project contract 274377: “Middle Atmosphere Dynamics: Exploiting Infrasound Using a Multidisciplinary Approach at High Latitudes (MADEIRA)”.

References

Amezcua, J., Näsholm, S.P., Blixt, E.M. and Charlton-Perez, A.J. (2020), Assimilation of atmospheric infrasound data to constrain tropospheric and stratospheric winds. QJR Meteorol. Soc. Accepted Author Manuscript.

Evers, L. G., & Schweitzer, J. (2011). A climatology of infrasound detections in northern Norway at the experimental ARCI array. Journal of seismology, 15(3), 473-486.

Blixt, E. M., Näsholm, S. P., Gibbons, S. J., Evers, L. G., Charlton-Perez, A. J., Orsolini, Y. J., & Kværna, T. (2019). Estimating tropospheric and stratospheric winds using infrasound from explosions. The Journal of the Acoustical Society of America, 146(2), 973-982. https://doi.org/10.1121/1.5120183

Diamond, M. (1964). Cross wind effect on sound propagation. Journal of Applied Meteorology, 3(2), 208-210.

Fomichev, V. I., Ward, W. E., Beagley, S. R., McLandress, C., McConnell, J. C., McFarlane, N. A., & Shepherd, T. G. (2002). Extended Canadian Middle Atmosphere Model: Zonal-mean climatology and physical parameterizations. Journal of Geophysical Research: Atmospheres, 107(D10), ACL-9.

Hedlin, M. A. H., Walker, K., Drob, D. P., & de Groot-Hedlin, C. D. (2012). Infrasound: Connecting the solid earth, oceans, and atmosphere. Annual Review of Earth and Planetary Sciences, 40, 327-354.

Liu, H. L., Bardeen, C. G., Foster, B. T., Lauritzen, P., Liu, J., & Lu, G. Wang, 339 W.(2018). Development and validation of the Whole Atmosphere Community 340 Climate Model with Thermosphere and Ionosphere Extension (WACCM-X 341 2.0). J. Adv. Model. Earth Syst, 10(2), 381-402.